Volume 1 | Number 1 | Jan 2013 | Pages 1–100

Journal of
Materials Chemistry A

Materials for energy and sustainability
www.rsc.org/materialsA

ROYAL SOCIETY
OF CHEMISTRY

ROYAL SOCIETY
OF CHEMISTRY

www.rsc.org/materialsA

Journal of Material Chemistry A

Dynamic Article Links ▶

ARTICLE

Efficient Polymer Solar Cells Based on Terpolymers with Broad Absorption Range of 300–900 nm

Yuanshuai Huang, Min Zhang, Huajie Chen, Fen Wu, Zhencai Cao, Lingjun Zhang, Songting Tan*

Three novel random conjugated terpolymers were designed and synthesized by copolymerizing benzo[1,2-*b*:4,5-*b'*]dithiophene (BDT) donor with a electron-deficient diketopyrrolo[3,4-*c*]pyrrole (DPP) unit and a thiophene-vinylene-dithienyl-benzothiadiazole (TVDTBT) side group in polymer backbone. By tuning the ratio of DPP and TVDTBT in terpolymers, the optical properties and energy levels of these random terpolymers can be rationally controlled. As a result, the terpolymers exhibited very broad absorption range of 300–900 nm
10 with high absorption coefficient and a deep HOMO energy level. Bulk heterojunction polymer solar cells fabricated from **P3** and PC$_{61}$BM exhibited a promising power conversion efficiency of 5.29% without any processing additives.

Introduction

In the past few years, polymer solar cells (PSCs) have attracted significant attention due to their potential application in low-cost,
15 light-weight, large-area, and flexible photovoltaic devices.[1–3] Recently, remarkable progresses have been made in this field, and the power conversion efficiencies (PCE) of PSCs have surpassed 10% as a result of the development of new conjugated polymers and improvements in the control over the morphologies
20 of bicontinuous interpenetrating electron donor/acceptor nanoscale networks.[4–5] And further improvements in many factors are needed for higher performance.[6–14]

The PCE of PSCs is the product of its short-circuit current density (J_{sc}), open-circuit voltage (V_{oc}) and fill factor (FF).
25 Whereas, a large portion of polymers are difficult to produce PCE over 6% due to the imbalance of the J_{sc} and V_{oc}.[15–16] To get high J_{sc} and V_{oc} simultaneously, one of the most effective approaches is the development of low band-gap conjugated polymers with broad absorption spectra as well as high absorption coefficient
30 and suitable energy levels matching with the electron acceptor (fullerene derivatives).[17–18] Generally, most of low band gap polymers exhibit a main absorption above 600 nm because of their strong intermolecular charge transfer (ICT) between donor and acceptor, but a weak absorption at 400–600 nm, therefore
35 decreasing the number of absorbed photons in the visible region and in turn limiting photocurrent.[19–20] To obtain broad and strong absorption in whole visible-near-infrared band, one promising approach is to develop random terpolymers by copolymerizing two different electron-deficient units with one electron-rich unit
40 to broaden the absorption of the solar spectrum.[21–22] Therefore, strategies to the design and synthesis of ideal terpolymers with a broad absorption and suitable HOMO energy levels are worthy of exploring.

Among high performance D–A polymer materials for PSCs,
45 benzo[1,2-*b*:4,5-*b'*]dithiophene (BDT) has been widely investigated and used as an electron-donating building-block, which attributes to its symmetric and planar conjugated structure.[23–25] Additionally, diketopyrrolo[3,4-*c*]pyrrole (DPP) has also been successfully used as a acceptor unit for high-
50 performance PSCs, because most of DPP-based D–A polymers exhibit a strong ICT absorption reaching 900 nm due to the presence of electron-deficient lactam rings.[26–28] While this series of polymers almost show a very weak absorption at 300–600 nm and high relatively HOMO energy levels. According to several
55 research groups and our previous studies, it had been demonstrated that polymers containing dithienylbenzodiathiazole (DTBT) side-group could obviously get a strong absorption at 300–600 nm and low HOMO energy levels due to a certain distortion of the polymer backbone.[29–36] Based on consideration
60 above, we introduced DTBT-containing side-group into random terpolymers, and synthesized three novel terpolymers **P1**, **P2**, and **P3** (**Scheme 1**). They exhibited very broad absorption rang of 300–900 nm and low HOMO energy level of -5.29eV ~ −5.47 eV. As a result, The PSC device based on **P3** show a high of 5.29%
65 (J_{sc}=14.47 mA cm^{-2}, V_{oc}=0.78 eV, FF=0.48) without any processing additives.
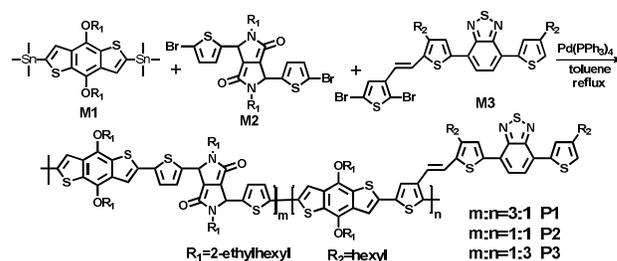
Scheme 1 Synthesis of the terpolymers **P1**, **P2**, and **P3**.

Experimental
70
Materials and methods

2,6-Di(trimethylstin)-4,8-di((2-ethylhexyl)oxy)benzo[1,2-*b*:4,5-

b′]dithiophene (M1), 2,5-diethylhexyl-3,6-bis(5-bromothiophene-2-yl)pyrrolo-[3,4-*c*]-pyrrole-1,4-dione (M2) were purchased from Derthon Optoelectronic Materials Science Technology Co Ltd (Shenzhen, China) and used without further purification. All other chemicals were purchased from Alfa Aesar. Tetrahydrofuran (THF) and toluene were dried and distilled from sodium/benzophenone and used directly. All other solvents and chemicals used in this work were analytical grade and used without further purification. Nuclear magnetic resonance spectra were measured with Bruker AVANCE 400 spectrometer. UV-visible absorption spectra of the polymers were conducted on a Perkin-Elmer Lamada 25 UV-Vis-NIR spectrometer. The average molecular weight and polydispersity index (PDI) of the polymers were determined using Waters 1515 gel permeation chromatography (GPC) analysis with THF as eluent and polystyrene as standard. Thermogravimetric analysis (TGA) measurement was conducted on a Netzsch TG 209 analyzer under nitrogen at a heating rate of 20 °C min^{-1}. Differential scanning calorimetry (DSC) analysis was made on a TA DSC Q10 instrument at a scan rate of 20 °C min^{-1}. Electrochemical redox potentials were obtained by cyclic voltammetry (CV) using a three-electrode configuration and an electrochemistry workstation (ZAHNER ZENNIUM) at a scan rate of 100 mV s^{-1}. CV was conducted on an electrochemistry workstation with the thin film on a Pt plate as the working electrode, Pt slice as the counter electrode, and saturated calomel electrode (SCE) as the reference electrode. The supporting electrolyte is 0.1 M tetra-n-butylammonium hexafluorophosphate (Bu$_4$NPF$_6$) in anhydrous acetonitrile solution. All AFM measurements were performed on a Digital Instruments Enviro Scope in a tapping mode.

Polymer Solar Cell Fabrication

The structure of the solar cells was ITO/MoO$_3$(20 nm)/Polymer:PC$_{61}$BM(~100 nm)/LiF(0.5 nm)/Al(100 nm). The PSCs devices were fabricated with indium oxides (ITO) glass as a positive electrode and LiF/Al as a negative electrode. The ITO glass was precleaned and then modified by a thin layer of MoO$_3$, which was deposited on ITO surface by vacuum evaporation under 3×10^{-7} Pa. The photosensitive layer was prepared by spin-coating a blend solution of polymer and [6,6]-phenyl C$_{61}$-butyric acid mmethyl ester (PC$_{61}$BM) in 1-chlorobenzene (CB) on the surface of ITO/MoO$_3$ substrate. Then, the LiF/Al cathode was deposited on the polymer layer by vacuum evaporation under 3×10^{-7} Pa. The accurate area of every device is 5.7 mm^2, defined by the overlap of the ITO and metal electrode. Current density-voltage (*J–V*) characteristics were measured by a Keithley 2602 Source Meter under 100 mW cm^{-2} irradiation using a 500W Xe lamp equipped with a global AM 1.5 filter for solar spectrum simulation. The incident light intensity was calibrated using a standard Si solar cell. The measurement of monochromatic incident photon-to-current conversion efficiencies (IPCE) was performed using a Zolix DCS300PA Data acquisition system.

Procedure for Synthesis of Monomers and Polymers

The synthetic routes for monomers and polymers are shown in **Scheme 1**. The monomer 4-(4-hexyl-2-thienyl)-7-[2-(2,5-dibromo-3-thienyl-vinyl)-4-hexyl-2-thienyl]-2,1,3-benzodiathiazole (M3) was synthesized according to literature procedures.[29]

Synthesis of **P1**: To a 25 mL three-neck round bottom flask, M1 (102.7 mg, 0.133 mmol), M2 (68.3 mg, 0.100 mmol), M3 (24.5 mg, 0.033 mmol), and dry toluene (10 mL) were added. The mixture was deoxygenated with nitrogen for 30 min. Then, Pd(PPh$_3$)$_4$ (15.4 mg, 0.013 mmol) was added under nitrogen and the reaction mixture was reacted for 48 h at 110 °C. After cooling to room temperature, the mixture was poured into 100 mL of methanol. A blue precipitate was collected by filtration. The product was purified by washing with methanol and hexane in a Soxhlet extractor for 24 h. It was extracted with hot chloroform in an extractor for 24 h. After removing solvent, a blue solid was collected (98.8 mg, 75.6%). ^{1}H NMR (400 MHz, CDCl$_3$, δ): 9.21–9.15 (br), 7.99–6.94 (br), 4.32–4.08 (br), 2.74–2.68 (br), 2.44–0.90 (br). M_n = 14.3 kg mol^{-1}, PDI = 1.92.

Synthesis of **P2**: Using a procedure similar to that described above for **P1**, a mixture of M1 (102.7 mg, 0.133 mmol), M2 (45.4 mg, 0.067 mmol), M3 (48.9 mg, 0.067 mmol) and Pd(PPh$_3$)$_4$ (15.4 mg, 0.013 mmol) in dry toluene (10 mL) was polymerized to give blue-red solid (95.6 mg, 72.3%). ^{1}H NMR (400 MHz, CDCl$_3$, δ): 9.21–9.15 (br), 7.99–6.94 (br), 4.32–4.08 (br), 2.74–2.68 (br), 2.44–0.90 (br). M_n = 17.1 kg mol^{-1}, PDI = 1.85.

Synthesis of **P3**: Using a procedure similar to that described above for **P1**, a mixture of M1 (102.7 mg, 0.133 mmol), M2 (22.7 mg, 0.033 mmol) M3 (73.2 mg, 0.100 mmol) and Pd(PPh$_3$)$_4$ (15.4 mg, 0.013 mmol) in dry toluene (10 mL) was polymerized to give red solid (99.4 mg, 74.3%). ^{1}H NMR (400 MHz, CDCl$_3$, δ): 9.21–9.15 (br), 7.99–6.94 (br), 4.32–4.08 (br), 2.74–2.68 (br), 2.44–0.90 (br). M_n = 16.6 kg mol^{-1}, PDI = 2.01.

Results and Discussion

Synthesis and Characterization

The terpolymers were synthesized via Stille coupling of M1, M2, and M3 monomer units in anhydrous toluene with a catalytic amount of Pd(PPh$_3$)$_4$, which were purified by Soxhlet extraction with ethanol, hexane, and chloroform. The resulting polymers exhibited excellent film-forming property and solubility in common organic solvents, including CB, THF and chloroform at room temperature, providing convenience for characterization and device processing. The number-average molecular weight (M_n) and polydispersity index (PDI) are 14.3 KDa and 1.92 for **P1**, 17.1 KDa and 1.85 for **P2**, and 16.6 KDa and 2.01 for **P3**, determined by gel permeation chromatography (GPC) with THF as an eluent. This similar molecular weight of polymers ensured more accurate comparisons between polymer structure and photophysical/photovoltaic properties.

Thermal properties

The terpolymers revealed high decomposition temperatures (T_d, 5% weight loss) of 378, 361, and 355 °C for **P1**, **P2**, and **P3**, respectively (Fig. 1). However it did not show any noticeable glass transition in differential scanning calorimetry (DSC) analysis in the temperature range from 40 °C to 300 °C. These results indicated that the terpolymers possess a good thermal and morphology stability which is a prerequisite for processing and
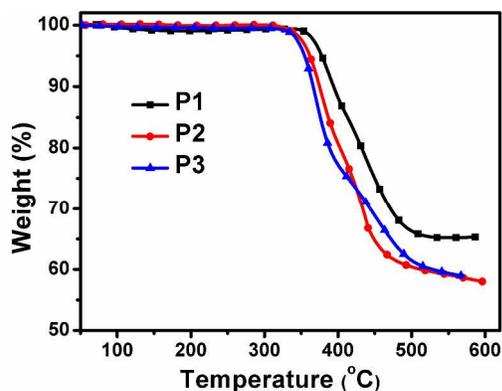
device application.

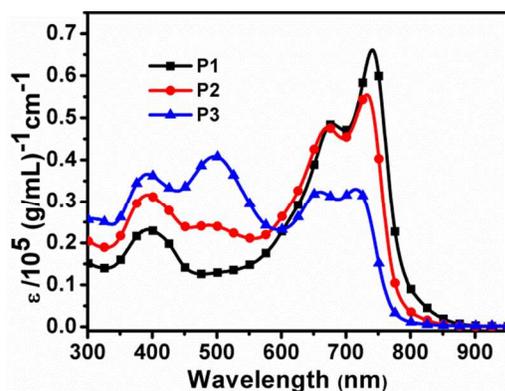

Fig. 1 TGA plot of the terpolymers

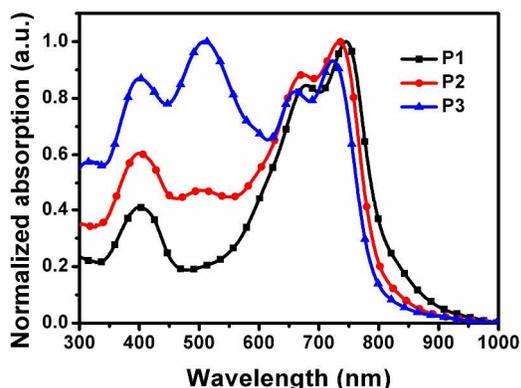Fig. 2 Absorption spectra of the terpolymers in dilute CHCl$_3$ solution (0.01 mg mL^{-1}).

Fig. 3 Absorption spectra of the terpolymers in thin film.

Optical properties

The UV-Vis-NIR absorption spectra of all terpolymers in dilute chloroform solution (0.01 mg mL^{-1}) and in thin film are shown in Fig. 2 and Fig. 3, respectively. All the random terpolymers in solution exhibited two or three obvious absorption bands (Table 1) ranging from 300 to 850 nm, a common feature of polymers based on donor and acceptor units. The first absorption band around 300–450 nm corresponds to the π–π* transition of the polymer backbone. The corresponding maximum absorption coefficients are 2.3, 3.2 and 3.7 ×10^4 g mL^{-1} cm^{-1} for **P1**, **P2** and

Table 1 Optical properties of the terpolymers.

Poly-mers	Solution λ_{max}(nm) (ε (10^4 g mL^{-1} cm^{-1}))	Film λ_{max} (nm)	λ_{edge} (nm)	E_g^{opt} (eV)
P1	391 (2.3), 677 (4.8), 741 (6.6)	400, 678, 746	867	1.43
P2	391 (3.2), 496 (2.4), 671 (4.8), 733 (5.5)	400, 504, 672, 734	842	1.47
P3	391 (3.7), 496 (4.1), 658 (3.2), 716 (3.3)	400, 509, 679, 723	821	1.52

P3, respectively. With elevating the contents of thiophene-vinylene-dithienyl-benzothiadiazole (TVDTBT), a new absorption band around 450–580 nm, as results the intermolecular charge transfer (ICT) bands from BDT to TVDTBT, became more clearly from **P1** to **P3** (1.3, 2.4, and 4.1 ×10^4 g mL^{-1} cm^{-1}, respectively). The absorption intensity between 300–600 nm was improved with increasing the contents of TVDTBT. While the ICT bands from BDT to DPP, around 580–820 nm (6.6, 5.5, and 3.3 ×10^4 g mL^{-1} cm^{-1} for **P1**, **P2**, and **P3**, respectively), gradually decreased, along with the increasing contents of TVDTBT. As expected, a strong and broad absorption ranging from 300–800 nm had been demonstrated for the as-synthesized terpolymer **P3**. This broad absorption would be favorable for high J_{sc}. Compared to their solution absorptions, all terpolymers thin films showed similar absorption peaks and broader absorption of 300–900 nm due to the stronger interchain aggregation. And a trend of the absorption onset was observed with a gradual blue-shift from **P1** to **P3**, along with higher TVDTBT content, which was due to the weaker electron-withdrawing character of TVDTBT compared to DPP. Note that **P3** with strong and broad absorption has great potential for increasing the photocurrent in PSCs. The optical band gaps (E_g^{opt}) of **P1**–**P3** are 1.43, 1.47 and 1.52 eV respectively, calculated from the onset of the film absorptions. By regulating the composition of the electron-deficient units, **P3** was observed from 300–820 nm, indicating that incorporating two different electron-deficient units into polymer is an effective method to control the optical band gap and broaden the absorption band.

Electrochemical properties

The electrochemical properties of the terpolymers were studied by cyclic voltammetry (CV) (Fig. 4 and Table 2). The potentials were referenced to the ferrocene/ferrocenium redox couple (Fc/Fc$^+$). The redox potential of Fc/Fc$^+$ was assumed an absolute energy level of –4.8 eV relative to vacuum, which was measured under the same condition as polymer sample to be 0.57 V related to the saturated calomel electrode (SCE). The corresponding HOMO and LUMO energy levels of polymers were calculated according to the equations: $E_{HOMO} = -e$ ($E_{ox} + 4.23$) (eV) and $E_{LUMO} = -e$ ($E_{red} + 4.23$) (eV). The HOMO levels of three terpolymers **P1**–**P3** were –5.29, –5.36, and –5.47 eV, respectively. We observe that increasing the contents of weak donor TVDTBT can lower the HOMO energy levels. As a result, P3 shows lowest the HOMO level of –5.47 eV, which is beneficial for obtaining high V_{oc} of PSCs and good air stability. For the LUMO levels of
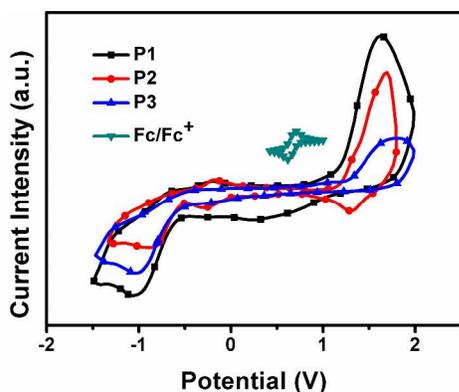
Fig. 4 Cyclic voltammograms curves of the terpolymers.

Table 2 Electrochemical properties of the terpolymers.

Polymers	E_{onset}^{ox} (V)	E_{onset}^{red} (V)	HOMO (eV)	LUMO (eV)	E_g^{ec} (eV)
P1	1.06	−0.53	−5.29	−3.70	1.59
P2	1.13	−0.54	−5.36	−3.69	1.67
P3	1.24	−0.56	−5.47	−3.67	1.80

all terpolymers is expected to mainly govern by the strongly electron–accepting DPP unit. LUMO levels were found to be in the range −3.70 to −3.67 eV, with the highest value −3.67 eV observed for P3, which contains the least amount of DPP. The LUMO energy level (−3.70 eV) is higher above 0.3 eV than $PC_{61}BM$ (−4.20 eV, measured under the same condition), suggesting that the charge transfer from the polymer to $PC_{61}BM$ would be effective. The electrochemical bandgap of the terpolymers is estimated to be 1.59, 1.67, and 1.80 eV, respectively, higher than their optical bandgap.

Polymer photovoltaic device characteristics

BHJ solar cells using the terpolymers (P1, P2, and P3) as the donors and $PC_{61}BM$ as an acceptor were investigated with the conventional device configuration. We investigated the performance of the PSC materials under a variety of conditions (Table 3 and Table 4). To avoid the influence of water vapor to PEDOT:PSS and enhance the photovoltaic properties, PSCs were fabricated with a $ITO/MoO_3(10$ nm)/polymer:$PC_{61}BM$/LiF(0.5 nm)/Al(100 nm) configuration.[37–38] The hole mobility of the target polymers was measured by using a space charge limit current (SCLC) method. Hole-only devices were fabricated with the configuration of ITO/PEDOT:PSS(30 nm)/Polymer:$PC_{61}BM$ (1:2)/MoO_3(10 nm)/Al(100 nm). The corresponding data of the terpolymers are summarized in Table 3. The weight ratio of polymer donor:$PC_{61}BM$ was optimized from 1:1 to 1:4 and the optimized weight ratio for three terpolymers and $PC_{61}BM$ was 1:2 (Table 4). Fig. 5 displays $J–V$ curves of the devices incorporating the terpolymers:$PC_{61}BM$ blends at a weight ratio of 1:2. We observe significant differences in performance between the three terpolymers. The devices prepared from P1–P3:$PC_{61}BM$ blends exhibited open circuit voltages (V_{oc}) of 0.72, 0.74, and
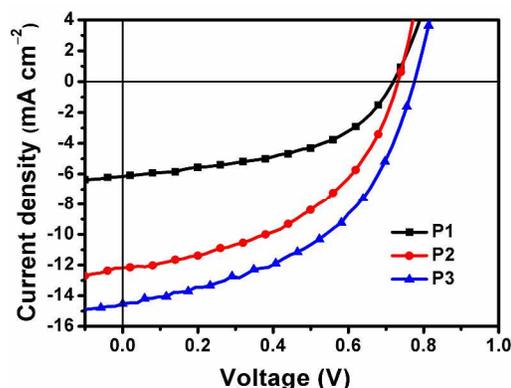

Fig. 5 $J–V$ curves of the photovoltaic cells based on the terpolymers:$PC_{61}BM$ (1/2, w/w).
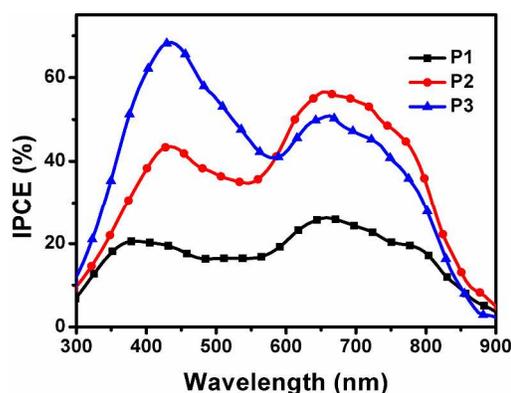

Fig. 6 IPCE curves of the photovoltaic cells based on the terpolymers:$PC_{61}BM$ (1/2, w/w).

0.78 eV, respectively. The short circuit current densities (J_{sc}) of the devices incorporating the **P3** blends (14.47 mA cm^{-2}) were greater than those of **P1** and **P2** (6.16 and 12.21 mA cm^{-2}, respectively); each value is related to the difference among the HOMO energy levels of the terpolymers. This high J_{sc} of **P3** matches well with its stronger light-harvesting ability covering from 300 to 900 nm. Therefore, the optimized **P3**:$PC_{61}BM$ devices, prepared at a blend weight ratio of 1:2, exhibited the hest PCE of 5.29% (J_{sc}=14.47 mA cm^{-2}, V_{oc}=0.78 eV, FF=0.48). Additionally, no further improvement can be observed by using 1,8-diiodooctane (DIO) as an additive and $PC_{71}BM$ as an acceptor (Table 4).

The spectra of incident photon-to-current conversion efficiencies (IPCE) were measured for the conventional BHJ cells with the 1:2 blend ratio of the terpolymers:$PC_{61}BM$ (Fig. 6), which are in approximate agreement with the values obtained from the $J–V$ characteristics. These devices exhibited significantly broad IPCE responses that extended from 300 to 900 nm corresponding absorbance of the active layers. The **P3** device exhibited a broad response over 40% from 350 to 750 nm, with a maximum value of 70% at 420 nm, consistent with its higher photocurrent.

To better understanding the relationship between PSCs performance and film microstructures, we have also investigated the morphologies of terpolymers (**P1**–**P3**)/$PC_{61}BM$ (1/2, w/w) blend by using atomic force microscopy (AFM) (Fig. 7). As is clearly evidenced by AFM height images, the **P3** film displays a

Table 3 Photovoltaic properties and hole mobilities of the terpolymers with terpolymers:PC$_{61}$BM blend ratio of 1:2 (w/w).

Polymers	J_{sc} (mA cm^{-2})	V_{oc} (V)	FF	PCE (%)	μ_h (cm^2 V^{-1} s^{-1})
P1	6.16	0.72	0.49	2.16	1.03×10^{-5}
P2	12.21	0.74	0.46	4.17	2.07×10^{-5}
P3	14.13	0.78	0.48	5.29	2.14×10^{-5}

Table 4 Performance details of PSC devices based on **P3**.

P3/PCBM (w/w)	DIO	J_{sc} (mA cm^{-2})	V_{oc} (V)	FF	PCE (%)
P3/PC$_{61}$BM=1:1	–	12.61	0.79	0.44	4.40
P3/PC$_{61}$BM=1:2	–	14.13	0.78	0.48	5.29
P3/PC$_{61}$BM=1:3	–	10.55	0.76	0.49	3.93
P3/PC$_{61}$BM=1:4	–	9.87	0.76	0.48	3.65
P3/PC$_{71}$BM=1:2	–	14.16	0.79	0.47	5.23
P3/PC$_{61}$BM=1:2	0.1%	7.16	0.77	0.45	2.44
P3/PC$_{61}$BM=1:2	1%	6.53	0.87	0.36	2.05
P3/PC$_{61}$BM=1:2	2%	3.74	0.58	0.33	0.70
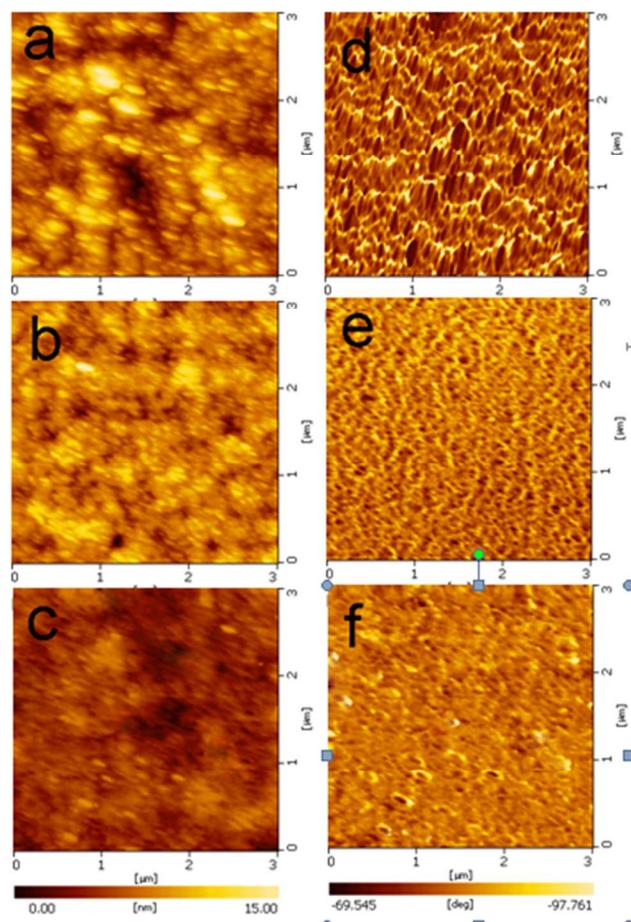
Fig. 7 AFM height images and phase images for terpolymers:PC$_{61}$BM blend films (w/w 1:2). (a) and (d): **P1**, (b) and (e): **P2**, (c) and (f): **P3**.

smooth and featureless image over the 3×3 μm^2 scan area, suggesting a relatively homogeneous morphology, that obviously precedes the images of **P1** and **P2**. From phase images of the terpolymers, we can observe the suitable phase separation in Figure 7 f. In short, by increasing the contents of TVDTBT, the J_{sc} value of **P3** was enhanced, which was correlated with their morphology and hole mobility.

Conclusions

We designed and synthesized three random conjugated terpolymers with different content DPP and TVDTBT side-group units for PSCs. The optical and electrochemical properties of the terpolymers were optimized by varying the ratio between DPP and TVDTBT in terpolymers. We found that, with increasing the contents of TVDTBT, the intensity of absorption band around 300–600 nm was improved and the HOMO levels get deeper. **P3** exhibited very complementary and broad absorption range of 300–800 nm with high absorption coefficient of 2.3 ×10^4 g mL^{-1} cm^{-1} in dilute solution and a deep-lying HOMO level (–5.47 eV), which are beneficial for achieving high J_{sc} and V_{oc}, respectively. As a result, polymer solar cells based on **P3**/PC$_{61}$BM blends (1/2, w/w) exhibited a high PCE of 5.29% (J_{sc}=14.47 mA cm^{-2}, V_{oc}=0.78 eV, FF=0.48) without any processing additives, indicating that the chemical structure of the conjugated random terpolymers has great potential for increasing J_{sc} and V_{oc} at the same time in bulk heterojunction photovoltaic devices.

Notes and references

College of Chemistry, and Key Laboratory of Environmentally Friendly Chemistry and Applications of Ministry of Education, and Key Laboratory of Advanced Functional Polymeric Materials of College of Hunan Province, Xiangtan University, Xiangtan 411105,China, E-mail: tanst2008@163.com

1   G. Yu, J. Gao, J. C. Hummelen, F. Eudl and A. J. Heeger, *Science*, 1995, **270**, 1789.
2   Y. J. Cheng, S. H. Yang and C. S. Hsu, *Chem. Rev.*, 2009, **109**, 5868.
3   J. M. Cao, Q. G. Liao, X. Y. Du, J. H. Chen, Z. Xia, Q. Q. Zuo and L. M. Ding, *Energy Environ. Sci.*, 2013, **6**, 3224.
4   J. You, L. Dou, K.Yoshimura, T. Kato, K. Ohya, T. Moriarty, K. Emery, C. Chen, J. Gao, G. Li, Y. Yang，*Nat. Commun.*,2013, **4**, 1446.
5   Z. He, C. Zhong, S. Su, M. Xu, H. Wu and Y. Cao, *Nat. Photonics*, 2012, **6**, 591.
6   M. He, F. Qiu and Z. Lin, *J. Phys. Chem. Lett.*, 2013, **4**, 1788.
7   W-L. Chan, M. Ligges, A. Jailaubekov, L. Kaake, L. Miajia-Avila and X-Y. Zhu, *Science*, 2011, **334**, 1541.
8   M. He, F. Qiu and Z. Lin, *J. Mater. Chem.*, 2011, **21**, 17039.
9   M. He, W. Han, J. Ge, Y. Yang, F. Qiu and Z. Lin, *Energy Environ. Sci.*, 2011, **4**, 2894.
10 A. Bhuwalka, J. F. Mike, M. He, J. J. Intemann, T. Nelson, M. D. Ewan, R. A. Roggers, Z. Lin and M. Jeffries, *Macromolecules*, 2011, **44**, 9611.
11 L. Chen, L. Huang, D. Yang, S. Ma, X. Zhou, J. Zhang, G. Tu and C. Li, *J. Mater. Chem. A*, 2014, DOI: 10. 1039/C3TA14396A.

12 F. Zhang, X. Xu, W. Tang. J. Zhang, Z. Zhuo, J. Wang, J. Wang, Z. Xu and Y. Wang, *Solar Energy Materials and Solar Cells*, 2011, **95**, 1785.

13 M. J. Zhang, Y. Gu, X. Guo, F. Liu, S. Q. Zhang, L. J. Huo, T. P. Russell and J. H. Hou, *Adv. Mater.*, 2013, **25**, 4944.

14 H. C. Chen, Y. H. Chen, C. C. Liu, Y. C. Chien, S. W. Chou, P. T. Chou, *Chem. Mater.*, 2012, **24**, 4766.

15 K. H. Hendriks, W. W. Li, M. M. Wienk and R. A. J. Janssen, *Adv. Energy Mater.*, 2013, **3**, 674.

16 H. Bronstein, E. C. Fregoso, J. R. Durrant and L. McCulloch, *Adv. Funct. Mater.*, 2013, **23**, 5647.

17 P. W. M. Blom, V. D. Mihailetchi, L. J. A. Koster and D. E. Markov, *Adv. Mater.*, 2007, **19**, 1551.

18 F. Liu, Y. Gu, J. W. Jung, W. H. Jo and T. P. Russell, *J. Polym. Sci. Part B: Polym. Phys.*, 2012, **50**, 1018.

19 X. Hu, L. Zou, W. Fu, T. T. Larsen-Olsen, M. Helgesen, E. Bundgaard, O. Hagemann, M. Shi, F. C. Krebs and H. J. Chen, *Mater. Chem.*, 2012, **22**, 15710.

20 E. Wang, J. Qi, Z. Wang, S. Hellstrom, F. Zhang, O. Inganas and M. R. Andersson, *Adv. Mater.*, 2010, **22**, 5240.

12 M. C. Yuan, M. Y. Chiu, C. M. Chiang and K. H. Wei, *Macromolecules*, 2010, **43**, 6270.

22 J. Li, K. H. Ong, P. Sonar, S. L. Lim, G. M. Ng, H. K. Wong, H. S. Tan and Z. K. Chen, *Polym. Chem.*, 2013, **4**, 804.

23 J. Hou, H. Y. Chen, S. Zhang, R. I. Chen, Y. Yang, Y. Wu and G. Li, *J. Am. Chem. Soc.*, 2009,**131**, 15586.

24 X. C. Wang, P. Jiang, Y. Chen, Z. G. Zhang, X. Y. Li, G. Yu and Y. F. Li, *Macromolecules.*, 2013, **46**, 4805.

25 C. Piliego, T. W. Holcombe, J. D. Douglas, C. H. Woo, P. M. Beaujuge and J. M. Frechet, *J. Am. Chem. Soc.*, 2010, **132**, 7595.

26 S. Q. Zhang, L. Ye, Q. Wang, Z. J. Li, X. Guo, H. L. Fan and J. H. Hou, *J. Phys. Chem. C*, 2013, **117**, 9550.

27 L. T. Dou, J. Gao, E. Richard, J. B. You, C. C. Chen, K. C. Cha, Y. J. He, G. Li and Y. Yang, *J. Am. Chem. Soc.*, 2012, **134**, 10071.

28 C. H. Duan, F. Huang and Y. Cao, *J. Mater. Chem.*, 2012, **22**, 10416.

29 Z. J. Gu, P. Shen, S. W. Tsang, Y. Tao, B. Zhao, P. Tang and S. T. Tan, *Chem. Commun.*, 2011, **47**, 9381.

30 Z. J. Gu, P. Tang, B. Zhao, H. Luo, X. Guo, H. Chen, G. Yu, X. Liu, P. Shen and S. T. Tan, *Macromolecules*, 2012, **45**, 2359.

31 H. Li, H. Luo, Z. Cao, Z. Gu, P. Shen, B. Zhao, H. Chen, G. Yu and S. Tan, *J. Mater. Chem.*, 2012, **22**, 22913.

32 J. H. Hou, Z. Tan, Y. Yan, Y. J. He, C. H. Yang and Y. F. Li, *J. Am. Chem. Soc.*, 2006, **128**, 4911.

33 E. Zhou, J. Z. Cong, K. Hashimoto and K. Tajima, *Energy Environ. Sci.*, 2012, **5**, 9756.

34 H. Tan, X. P. Deng, J. T. Yu, B. F. Zhao, Y. F. Wang, Y. Liu, W. G. Zhu, H. B. Wu and Y. Cao, *Macromolecules*, 2013, **46**, 113.

35 C. W. Wang, B. Zhao, Z. C. Cao, P. Shen, Z. Tan, X. L. Li and S. T. Tan, *Chem. Commun.*, 2013, **49**, 3857.

36 X. S. Liu, Y. S. Huang, Z. C. Cao, C. Weng, H. J. Chen and S. T. Tan, *Polym. Chem.*, 2013, **4**, 4737.

37 F. M. Liu, S. Y. Shao, X. Y. Guo, Y. Zhao and Z. Y. Xie, *Sol. Energy Mater. Sol. Cells*, 2010, **94**, 842.

38 C. B. Nielsen, R. S. Ashraf, B. C. Schroeder, P. D. Angelo, S. E. Watkins, K. Song, T. D. Anthopoulos and L. McCulloch, *Chem. Commun.*, 2012, **48**, 5832.